# BASIC PROPERTIES OF STARS. III: MASS

## 4.1 Introduction

It was stated earlier that the most important property of a star is its mass. Stellar masses can be determined directly by studying their gravitational interaction with other objects. As at least half of all (nearby) stars are thought to be in multiple systems, there are many opportunities to monitor the motions of binary stars to deduce their masses. Considering for simplicity only binary stars (as opposed to triple and quadruple systems), we distinguish three main classes: visual binaries, eclipsing binaries and spectroscopic binaries. We now consider them in turn.

## 4.2 Visual Binaries

Visual binaries tend to be systems that are relatively close to us so that the individual stars can be resolved. They are systems in which the component stars are also physically widely separated, tens to a few hundred AUs. The stars in such systems are gravitationally bound to each other but otherwise do not 'interact' as do other close binaries where one star may draw material off the surface of the other. The brightest component in the system has the suffix "A", the next "B" and so on. Systems with three or four components have been identified. Less than 1,000 visual binary systems have been detected. Two out of the three brightest stars in the sky, $\alpha$ CMa and $\alpha$ Cen, are binaries.

Referring to Figure 4.1, with the two stars orbiting about the common centre of mass, we have straightforwardly:

$$\frac{m_1}{m_2} = \frac{r_2}{r_1} = \frac{a_2}{a_1} \tag{4.1}$$

where $m$ is the stellar mass, $r$ is the star's distance from the centre of mass and $a$ is the semi-major axis of the elliptical orbit. By monitoring over the years (provided the period is not too long compared to human

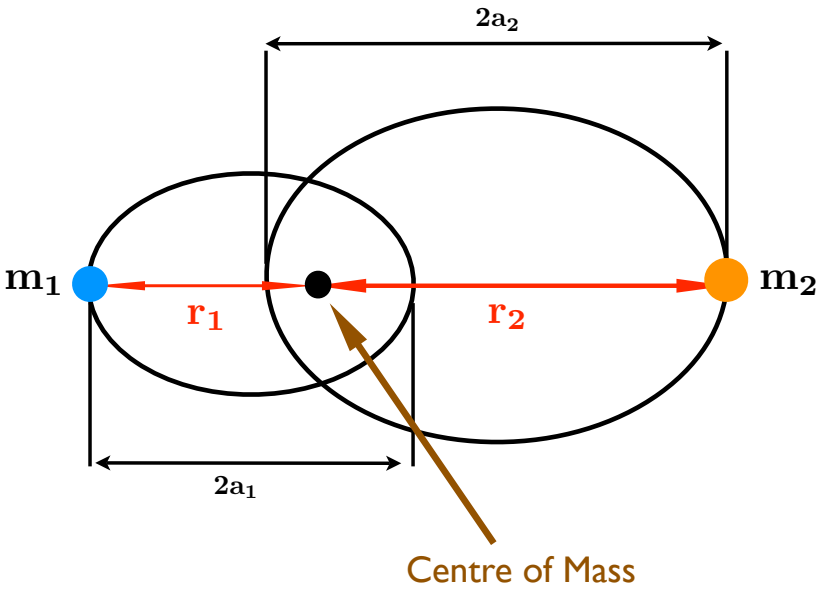


Figure 4.1: Schematic of a binary star system viewed face-on. In this example, $m_1 = 2\,m_2$.

timescales!) the relative positions on the sky of the two stars, it is possible to determine the orientation of the orbits and the system's centre of mass (see Figure 4.2). The distances $r_1$, $r_2$ from the common centre of mass subtend angles $\theta_1 = r_1/d$ and $\theta_2 = r_2/d$ at the star's distance $d$. It is therefore possible to deduce the mass ratio immediately from observations of the orbits:

$$\frac{m_1}{m_2} = \frac{\theta_2}{\theta_1} \tag{4.2}$$

If we know $d$, for example from parallax measurements, we can deduce the

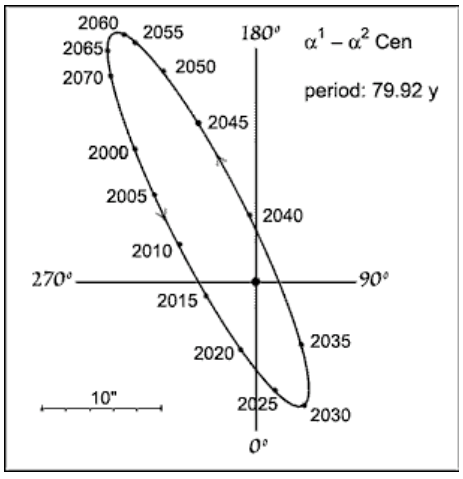


Figure 4.2: Sky projection of the orbit of $\alpha$ Cen B relative to $\alpha$ Cen A. The predicted positions of B relative to A for the current orbit are shown by year.

individual masses using Kepler's third law:

$$P^2 = \frac{4\pi^2}{G\,(m_1 + m_2)}\,a^3 \tag{4.3}$$

where $P$ is the period (the same for both orbits) and $a = a_1 + a_2$ is the semimajor axis of the orbit of the reduced mass $\mu$,

$$\mu = \frac{m_1 \cdot m_2}{m_1 + m_2}\,.$$

Recall that, in general, a two-body problem may be treated as an equivalent one-body problem with the reduced mass $\mu$ moving about a fixed mass $M = m_1 + m_2$ at a distance $r = |\mathbf{r}_2 - \mathbf{r}_1|$.

In order to deduce $m_1$ and $m_2$ from observations of $\theta_1$, $\theta_2$ and $P$ it is necessary to correct for: (i) the parallax of the whole system, (ii) the proper motion of the centre of mass, and (iii) the inclination of the plane of the orbit relative to the plane of the sky. (i) is easy: just observe a binary system for more than one year cycle. (ii) is also relatively simple, since the centre of mass must move at constant velocity. (iii) is trickier.

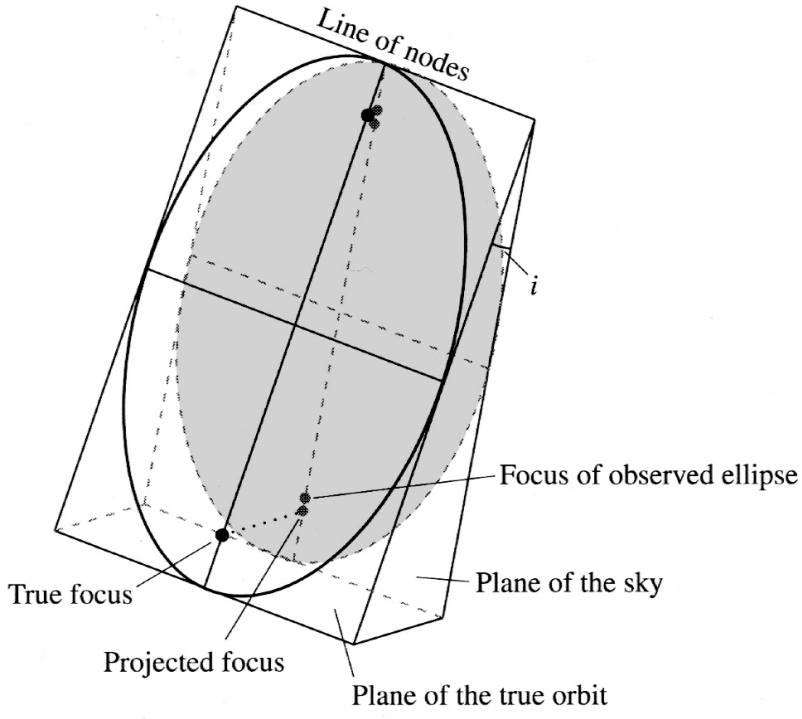


Figure 4.3: The projection of an elliptical orbit inclined by the angle $i$ to the plane of the sky is also an elliptical orbit. However, the real foci of the ellipse do not project to the foci of the observed ellipese. (Reproduced from Carroll & Ostlie's *Modern Astrophysics*).

Consider the special case where the orbital plane is inclined at angle $i$ to the plane of the sky (that is, it is inclined by an angle $90° - i$ to the line of sight) and the two planes intersect along a line parallel to the minor axis of the stellar orbit, forming a *line of nodes*, as in Figure 4.3. What we observe in this case are angles $\theta_1' = \theta_1 \cos i$ and $\theta_2' = \theta_2 \cos i$. The unknown inclination doesn't affect the estimate of the mass ratio, since the $\cos i$ factors cancel out in eq. 4.2. However, they can make a significant difference in the estimate of $a$ in eq. 4.3, which now becomes (solving for the sum of the masses):

$$m_1 + m_2 = \frac{4\pi^2}{G} \frac{(\theta d)^3}{P^2} = \frac{4\pi^2}{G} \left(\frac{d}{\cos i}\right)^3 \frac{\theta'^3}{P^2} \tag{4.4}$$

where $\theta$ is in radians and $\theta' = \theta_1' + \theta_2'$.

Thus, in order to evaluate the sum of the masses properly, we need to know the angle of inclination $i$. This can be deduced by careful observation of the centre of mass which, as shown in Figure 4.3, will not coincide with the the focus of the projected ellipse. The geometry of the true ellipse may be determined by comparing the observed stellar positions with mathematical projections of various ellipses onto the plane of the sky. The real situation is of course more complicated because in general the orbital plane may be inclined about both the minor and major axes.

In cases where the distance to a visual binary is not known, it may still be possible to deduce $a_1$ and $a_2$ and solve for $m_1$ and $m_2$ using radial velocity measurements, which give the projections of the velocity vectors along the line of sight.

Several hundred visual pairs are known, but in most cases it has not yet been determined whether they are bound binary systems or chance superpositions. Many visual binaries have long orbital periods of several centuries or millennia and therefore have orbits which are uncertain or poorly known. For this reason, they only sample rather sparsely the HR diagram, with a strong bias towards the more common (and therefore more likely to occur in the solar vicinity) low mass stars. Fortunately, other types of binary stars help us expand the range of reliable stellar mass determinations.

## 4.3 Spectroscopic Binaries

When two stars in a binary system are too far away to be resolved even with the largest telescopes on Earth, the binarity of the system can still be inferred from consideration of the spectrum, which will be the superposition of two sets of spectral features (which may be different if the stars are of different spectral types). In *double-lined spectroscopic binaries*, the absorption lines in the composite spectrum will be seen to move in wavelength, as each star moves in its orbit towards us and away from us (see Figure 4.4). The maximum blueshift and redshift we measure within an orbit are lower limits to the true velocities because of the unknown inclination $i$ of the orbital plane to the line of sight: $v_1 r_{\max} = v_1 \sin i$ and $v_2 r_{\max} = v_2 \sin i$.

Many spectroscopic binaries have nearly circular orbits because the timescales of tidal interactions which tend to circularise the orbits are short compared to the stellar lifetimes. When the eccentricities are small ($\epsilon \ll 1$), the orbital speed is essentially constant: $v = 2\pi a/P$ and where $P$ is the period

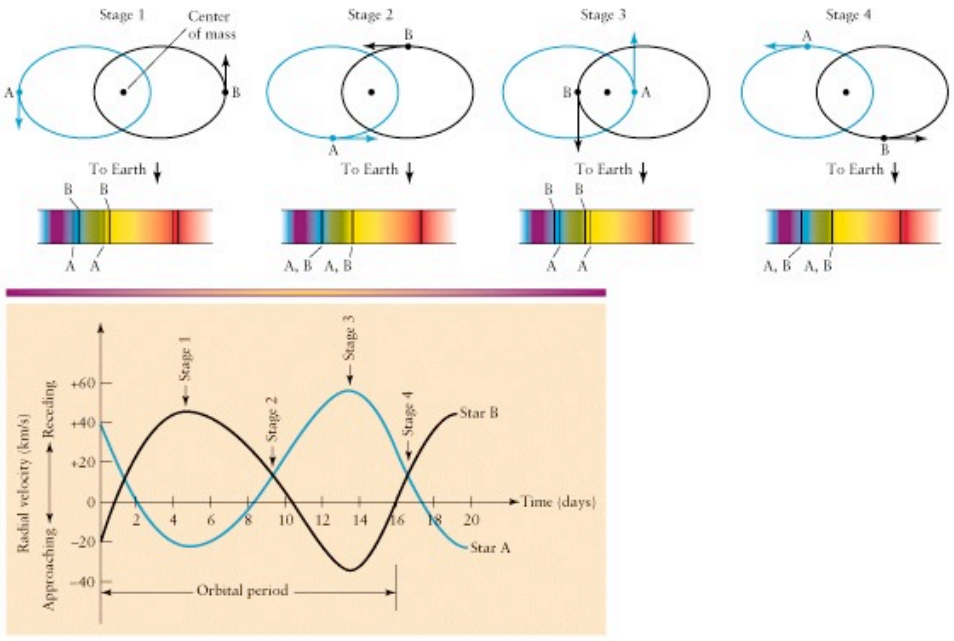


Figure 4.4: Schematic diagram of a double-lined spectroscopic binary, showing the orbits and the resultant composite spectrum produced at different orbital phases. Note that the centre of mass of the system has a radial velocity $v_r \simeq +15\,\mathrm{km\ s^{-1}}$ .

and the semi-major axis $a$ is now the radius. Substituting into eq. 4.1, we now have:

$$\frac{m_1}{m_2} = \frac{v_2}{v_1} \tag{4.5}$$

or, in terms of the observables:

$$\frac{m_1}{m_2} = \frac{v_{2r}/\sin i}{v_{1r}/\sin i} = \frac{v_{2r}}{v_{1r}}. \tag{4.6}$$

Thus, as in the case of visual binaries, the mass ratio can be deduced independently of the unknown inclination angle $i$.

However, the sum of the masses does require knowledge of $\sin i$. Replacing $a$ with:

$$a = a_1 + a_2 = \frac{P}{2\pi}\,(v_1 + v_2)\,, \tag{4.7}$$

substituting into eq. 4.3 and solving for the sum of the masses, we obtain:

$$m_1 + m_2 = \frac{P}{2\pi G}\,(v_1 + v_2)^3\,, \tag{4.8}$$

or, in terms of the observables:

$$m_1 + m_2 = \frac{P}{2\pi G}\,\frac{(v_{1r} + v_{2r})^3}{\sin^3 i}. \tag{4.9}$$

Since the inclination angle is generally unknown, eq. 4.9 is usually solved statistically. That is, we assume that the orbits are randomly inclined relative to our line of sight and use the integral average of $\sin^3 i$ between 0 and 90°, $(\langle \sin^3 i \rangle) = 3\pi/16 \simeq 0.589$, to deduce the average mass of stars in a given luminosity or $T_{\rm eff}$ class. A selection effect correction is usually applied to account for the fact that when the orbits are nearly face-on ($i$ less than a few degrees, $\sin i \ll 0.1$), it is much more difficult to recognise that a star is a spectroscopic binary. Thus the larger value $(\langle \sin^3 i \rangle) \simeq 2/3$ is usually taken to be representative in this statistical approach.

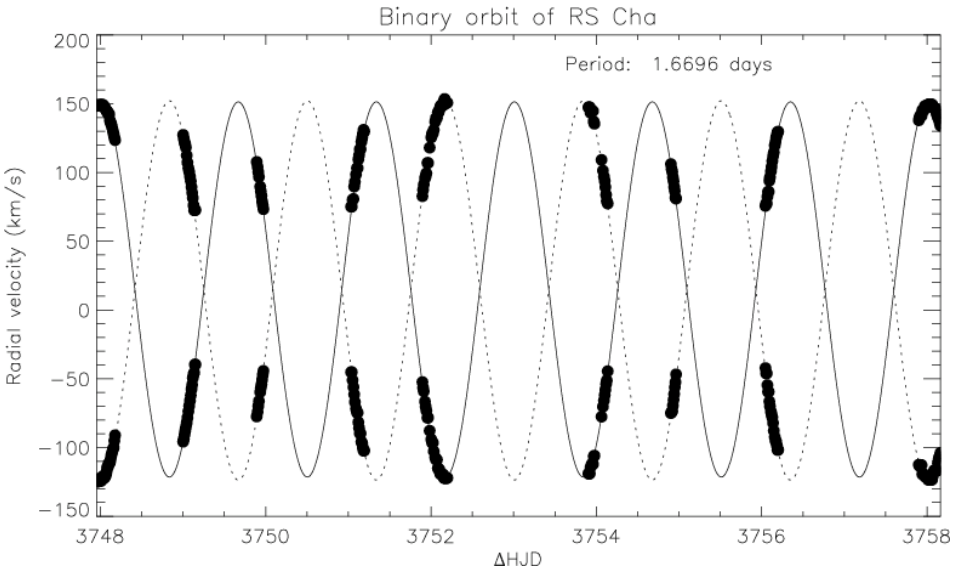


Figure 4.5: RS Cha belongs to an enigmatic group of pre-main sequence (PMS) stars of intermediate mass, between 2 and 8 $M_\odot$, referred to as Herbig Ae/Be stars from the American astronomer who first identified them in 1960. At a parallactic distance of $93 \pm 2$ pc, RS Cha is a bright spectroscopic eclipsing binary star, with both components being Herbig Ae PMS stars of similar mass ($\sim 1.9 M_\odot$). Their age is $6^{+2}_{-1}$ Myr; other physical parameters are collected in Table 4.1. This Figure, reproduced from Böhm et al. (2009), shows the radial velocities of the two stars measured with near-continuous observations during 14 nights at the 1 m Mt John (New Zealand) telescope using a high resolution spectrograph. Note the sinusoidal velocity curves, indicative of nearly circular orbits. The orbital plane lies close to our line of sight ($i = 83.4$); thus, the measured values of $v_{1r}$ and $v_{2r}$ are very close to the real velocities $v_1$ and $v_2$ ($\sin i = 0.99$).

**Table 4.1.** Parameters of RS Cha. References: [1] Alecian et al., 2005, [2] Ribas et al., 2000, [3] Clausen & Nordstrom, 1980.

| Parameter | Primary | Secondary | References |
|---|---|---|---|
| $M/\mathrm{M}_\odot$ | 1.89±0.01 | 1.87±0.01 | [1] |
| $R/\mathrm{R}_\odot$ | 2.15±0.06 | 1.87±0.01 | [1] |
| $T_{\rm eff}$ [K] | 7638±76 | 7228±72 | [2] |
| $\log(L/\mathrm{L}_\odot)$ | 1.15±0.09 | 1.13±0.09 | $L = 4\pi R^2 \sigma T_{\rm eff}^4$ |
| $\log(g)$ [cm s$^{-2}$] | 4.05±0.06 | 3.96±0.06 | $g = M\mathrm{G}/R^2$ |
| $v \sin i$ [km s$^{-1}$] | 64±6 | 70±6 | [1] |
| $P_{\rm orb}$ [d] | 1.67 | | [1] |
| $i$ [deg] | 83.4±0.3 | | [3] |
| [Fe/H] | 0.17±0.01 | | [1] |

Of much interest in astronomy are *single-lined spectroscopic binaries*. These are cases where only the spectrum of one of the pair is observed, but the periodic variations in its radial velocity indicate the presence of an unseen companion. This could be the case if: (a) the second star is very much fainter than the first—Sirius A and B are a good example; (b) the companion is a dark object, such as a neutron star or a black hole—such systems provide some of the most compelling evidence for the existence of stellar-mass black holes; and (c) if the secondary is a planet. In this case, the radial velocity amplitudes are only m $s^{-1}$, rather than km $s^{-1}$.

In single-lined binaries, where we cannot measure $v_{2r}$, we can substitute the relation $v_{2r} = v_{1r}m_1/m_2$ (eq. 4.6) into eq. 4.9 to obtain:

$$m_1 + m_2 = \frac{P}{2\pi G} \frac{v_{1r}^3}{\sin^3 i} \left(1 + \frac{m_1}{m_2}\right)^3 \tag{4.10}$$

which can be rearranged in a form which groups together all the observables on the right-hand side of the equation:

$$\frac{m_2^3}{(m_1 + m_2)^2} \sin^3 i = \frac{P}{2\pi G} v_{1r}^3. \tag{4.11}$$

The left-hand side of this equation is known as the mass function. Even if $m_1$ is not known, the mass function can still provide interesting lower limits to the mass of the unseen companion, since $m_1 > 0$ and $\sin i \leq 1$, and therefore:

$$\frac{P}{2\pi G} v_{1r}^3 < m_2 \tag{4.12}$$

If the condition $m_2 \ll m_1$ is satisfied, which is the case of the secondary component of the binary system is a planet, then $m_1 + m_2 \approx m_1$. Substituting into 4.11, we now have:

$$m_2^3 \sin^3 i \approx \frac{P}{2\pi G} v_{1r}^3 m_1^2 \tag{4.13}$$

While there is still an inclination uncertainty for any particular system, statistical results can be obtained for large sample of stars with measured oscillations attributable to planet-mass companions.

## 4.4 Eclipsing Binaries

The ambiguities associated with the unknown orientation can be removed in cases where we see occultations of one of the stars by the other. Provided that the separation between the two stars is much greater than the sum of their radii (a condition which is *not* satisfied in contact binaries), then it must be the case that the inclination of the orbital plane to the sky is close to 90° (see Figure 4.6). Note also that for $i > 75°$, $\sin i > 0.9$, so that the error in the masses deduced with the assumption that $i = 90°$ is less than 10%.

Comparing the light curves for the cases of complete (Figure 4.6) and partial (Figure 4.7) eclipse, it can be appreciated that it is possible to recognise the cases where $i < 90°$.

When the eclipse is total, we can deduce the radii of both stars from accurate timing of the phases of the eclipse. With the assumption that the smaller star is moving perpendicularly to our line of sight during the duration of the eclipse, its radius can be straightforwardly derived from

$$r_s = \frac{v}{2}\,(t_b - t_a) \tag{4.14}$$

where $t_a$ and $t_b$ are the times of first contact and minimum light respectively (see Figure 4.6) and $v = v_s + v_l$ is the relative velocity of the two stars.

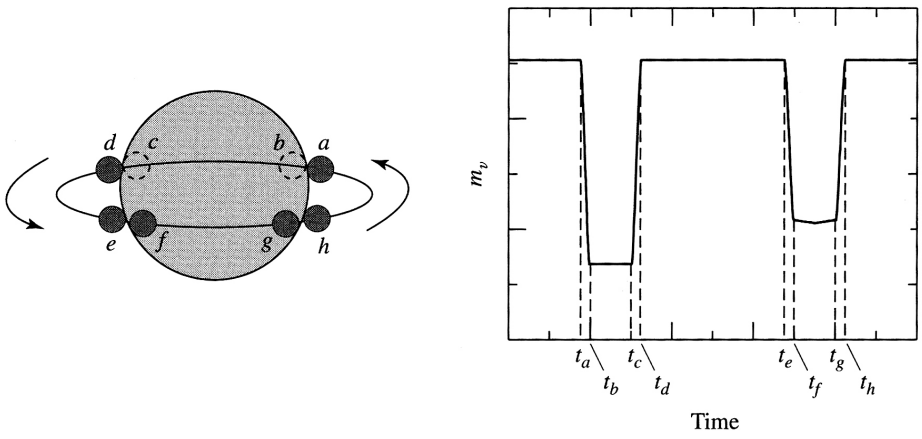


Figure 4.6: Schematic diagram of an eclipsing binary. The smaller star is assumed to be hotter than the larger one. (Reproduced from Carroll & Ostlie's *Modern Astrophysics*).

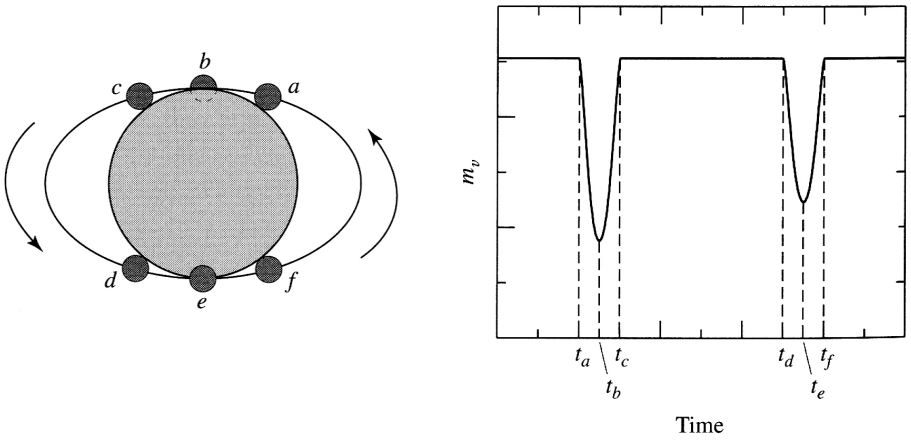


Figure 4.7: Schematic diagram of a partial eclipsing binary. The smaller star is assumed to be hotter than the larger one. (Reproduced from Carroll & Ostlie's *Modern Astrophysics*).

Similarly:

$$r_l = \frac{v}{2}\,(t_c - t_a) \;=\; r_s + \frac{v}{2}\,(t_c - t_b) \tag{4.15}$$

The light curve of eclipsing binaries gives information not only on the radii of the two stars but also on the ratio of their effective temperatures. This follows directly from eq. 2.13, $L = 4\pi R^2 \sigma T^4$; as when an area $\pi R^2$ is eclipsed from the system, the drop in flux will be different depending on whether the hotter star of the two is in front or behind the cooler one (see Figure 4.6). Assuming for simplicity a uniform flux across the stellar disk, we have:

$$F_0 = A\left(\pi R_l^2 F_l' + \pi R_s^2 F_s'\right) \tag{4.16}$$

where $F'$ is the radiative surface flux, $F_0$ is the measured flux when there is no eclipse, and $A$ is a proportionality constant to account for the fact that we register only a fraction of the flux emitted (due to distance, intervening absorption and limited efficiency of the instrumentation). The deeper, or primary, minimum in the light curve occurs when the hotter star is eclipsed by the cooler one. In the example shown in Figure 4.6, this is the smaller star. Then, during the primary minimum we have:

$$F_1 = A\pi R_l^2 F_l' \,, \tag{4.17}$$

while during the secondary minimum:

$$F_2 = A\left(\pi R_l^2 - \pi R_s^2\right) F_l' + A\pi R_s^2 F_s' \,. \tag{4.18}$$

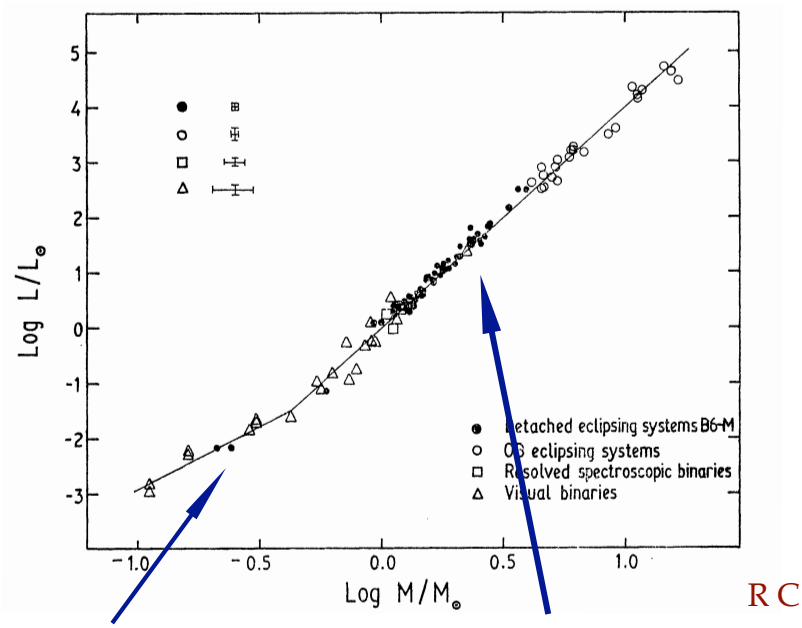


Figure 4.8: The empirical stellar mass-luminosity relation constructed from observations of different types of binary stars (from Smith 1983).

To circumvent uncertainties in the constant $A$, we concern ourselves with the ratio of the two fluxes:

$$\frac{F_0 - F_1}{F_0 - F_2} = \frac{F'_s}{F'_l} = \left(\frac{T_s}{T_l}\right)^4 \tag{4.19}$$

What eq. 4.19 tells us is that the ratio of the measured fluxes during the primary and secondary eclipses gives a direct measure of the ratio of the effective temperatures of the two stars in the eclipsing binary system.

## 4.5 The Stellar Mass-Luminosity Relation

When we bring together the best determinations of stellar masses from different types of binary stars, we find a well defined mass-luminosity relation for hydrogen burning dwarfs. Figure 4.8 shows the empirical mass-luminosity relation constructed from data available in the late 1970s-early 1980s. Thirty years later, the number of stars with direct measurements of mass and radius has increased considerably, thanks in part to the advent of long-baseline optical interferometry which can resolve the stellar disks. Figure 4.9, reproduced from the review by Torres et al. 2010 (A&ARv,

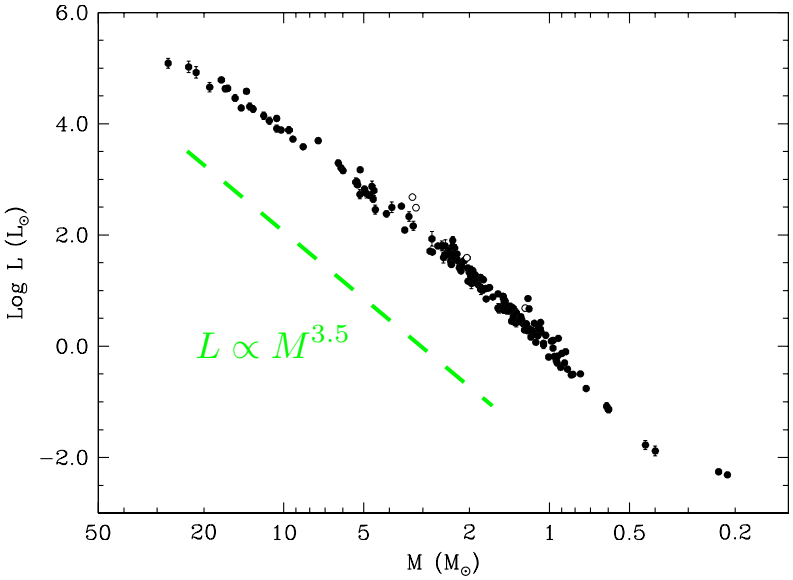


Figure 4.9: The empirical stellar mass-luminosity relation from observations of 190 stars in 95 detached binary systems, all with masses and radii known with an accuracy of 3% or better (data from Torres et al. 2010).

18, 67), is a compilation of measurements for 95 detached binary systems containing 190 stars satisfying the criterion that the mass and radius of both stars be known with an accuracy of 3% or better.

Any theory of stellar structure must be able to reproduce such a relation in order to be deemed valid; we shall return to this point in Lecture 10. Here we limit ourselves to some preliminary considerations. First of all, such a clear-cut $M - L$ relation provides a natural explanation for the existence of a prominent main sequence in the HR diagram. After forming within a collapsing interstellar cloud, stars begin their hydrogen-burning lives on the main sequence, at a location on the $M_V$–$(B-V)$ plane *determined by their mass*. Stars do *not* evolve along the main sequence, they evolve *off* the main sequence.

A rough approximation to the slope of the mass-luminosiy relation over the full range of stellar masses is $L \propto M^{\sim 3.5}$. If stars shine through nuclear fusion, we can write:

$$\frac{dM}{dt} = k\,L$$

where $L$ is the luminosity and $k$ is a constant of proportionality. Integrating, we have:

$$t \propto \frac{M}{L} \propto \frac{M}{M^{3.5}} \propto M^{-2.5}\,.$$

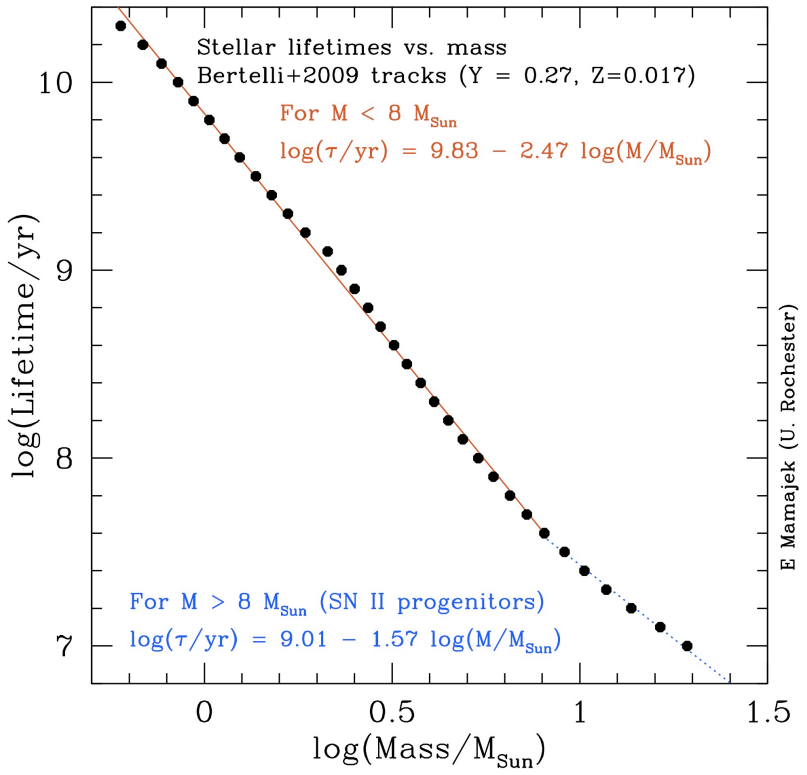


Figure 4.10: Stellar lifetimes as a function of mass from the stellar evolution models of Bertelli et al. (2009). Stars more massive than $8M_{\odot}$ (with lifetimes $t < 4 \times 10^7$ years) are thought to end their lives as Type II supernovae.

In other words, the steep slope of the stellar mass-luminosity relation implies a very strong dependence of the stellar lifetimes on their mass. While a $1M_{\odot}$ star will burn hydrogen for $10^{10}$ years before evolving off the main sequence, a $20M_{\odot}$ star has sufficient fuel to last for only $10^7$ years (see Figure 4.10).